J.M. Vasco-Olmo et alii, Frattura ed Integrità Strutturale, 41 (2017) 166-174; DOI: 10.3221/IGF-ESIS.41.23

Focused on Crack Tip Fields

Experimental methodology for the quantification of crack tip plastic zone and shape from the analysis of displacement fields

J.M. Vasco-Olmo, F.A. Díaz
University of Jaén, Spain
jvasco@ujaen.es
fdiaz@ujaen.es

M.N. James, C.J. Christopher
University of Plymouth, UK
M.James@plymouth.ac.uk
C.Christopher@plymouth.ac.uk

E.A. Patterson
University of Liverpool, UK
Eann.Patterson@liverpool.ac.uk

ABSTRACT. The current work presents a novel methodology for the experimental quantification of the crack tip plastic zone during fatigue crack growth. This methodology is based on the application of yield criteria to estimate the area and the shape of the plastic zone at the crack tip. The implementation of the proposed methodology requires the use of strain maps calculated from the differentiation of the displacement fields obtained by digital image correlation (DIC). Stress maps can subsequently be inferred from both von Mises and Tresca yield criteria. Fatigue tests and associated measurements of plastic zone size and shape were conducted on a compact-tension specimen made from commercially pure titanium at *R* ratio of 0.6. In addition, the ability to predict the shape and size of the experimentally observed crack tip plastic zone has been explored using three different analytical elastic crack tip models [Westergaard, Williams and Christopher-James-Patterson (CJP)]. This analysis indicated that the CJP model provided the most accurate prediction of the plastic zone and shape.

KEYWORDS. Crack tip plastic zone; Fatigue; Crack tip fields; Crack shielding; Stress intensity factor, DIC.

Citation: Vasco-Olmo, J.M., Díaz, F.A., James, M.N., Christopher, C.J., Patterson, E.A., Experimental methodology for the quantification of crack tip plastic zone and shape from the analysis of displacement fields, Frattura ed Integrità Strutturale, 41 (2017) 166-174.

Received: 28.02.2017
Accepted: 15.04.2017
Published: 01.07.2017

INTRODUCTION

It has long been recognised in the fracture mechanics community that identifying plastic zone shape and size, and any influences of the plastic zone on a growing fatigue crack is relatively complex whether attempted by simulation or experiment. In simulation work, predictions are usually based on a purely elastic theoretical modelling of crack tip stress fields. Experimentally, determination of the plastically deformed region surrounding a growing fatigue crack has been pursued using a variety of techniques to identify the dimensions of crack tip plastic zones. Uguz and Martin [1] provide a useful review of the early experimental work on characterising the crack tip plastic zone; this includes techniques based on microhardness measurements, etching, optical interference, micro-strain gauge and electron microscopy. Modern numerical modelling techniques and advanced experimental techniques, including synchrotron diffraction and tomography [2], digital image correlation (DIC) [3], thermography [4] and electron backscatter diffraction (EBSD) [5] have started to unlock the potential of full-field measurements in determining crack tip stress intensity factors, residual stresses, strains and hence plastic zone dimensions.

Most of the reported works to predict plastic zone size and shape at the crack tip employ approaches based on Linear Elastic Fracture Mechanics (LEFM), such as Irwin' [6] or Dugdale's [7] estimates, or the model based on Westergaard equations [8], among others. However, these are simplistic approaches and, therefore there is a clear application field consisting in combining full field measurement techniques with an improved model of the crack tip stress field that attempts to better incorporate the influence on the elastic stress field driving growth, of any stresses induced by the plastically deformed region that surrounds a growing fatigue crack.

The objective of the current work is the experimental determination of the plastic zone size and shape by using DIC in titanium compact tension specimens, and then to evaluate the capability of three crack tip field models to characterise stress or displacement and hence to predict plastic zone size and shape. The three models considered in this work are the Westergaard crack tip stress equations, Williams' expansion series for crack tip stresses and the recently developed CJP model [9] for crack tip displacement fields.

DESCRIPTION OF THE MODELS FOR THE CHARACTERISATION OF CRACK TIP FIELDS

WESTERGAARD EQUATIONS

According to the Westergaard equations, the stress field around the crack tip [8] is described using the stress intensity factors (SIFs), K_I and K_{II}, the T-stress (T) and a polar coordinate system with its origin at the crack tip. Crack tip stress fields are then defined as:

$$\begin{Bmatrix}\sigma_x\\ \sigma_y\\ \tau_{xy}\end{Bmatrix}=\frac{K_I}{\sqrt{2\pi r}}\cos\frac{\theta}{2}\begin{Bmatrix}1-\sin\frac{\theta}{2}\sin\frac{3\theta}{2}\\ 1+\sin\frac{\theta}{2}\sin\frac{3\theta}{2}\\ \sin\frac{\theta}{2}\cos\frac{3\theta}{2}\end{Bmatrix}+\frac{K_{II}}{\sqrt{2\pi r}}\begin{Bmatrix}-\sin\frac{\theta}{2}\left(2+\cos\frac{\theta}{2}\cos\frac{3\theta}{2}\right)\\ \sin\frac{\theta}{2}\cos\frac{\theta}{2}\sin\frac{3\theta}{2}\\ \cos\frac{\theta}{2}\left(1-\sin\frac{\theta}{2}\sin\frac{3\theta}{2}\right)\end{Bmatrix}+\begin{Bmatrix}T\\0\\0\end{Bmatrix} \quad (1)$$

In a similar way, crack tip displacement fields [8] are described as:

$$\begin{Bmatrix}u\\ v\end{Bmatrix}=\frac{K_I}{2G}\sqrt{\frac{r}{2\pi}}\begin{Bmatrix}\cos\frac{\theta}{2}\left(\kappa-1+2\sin^2\frac{\theta}{2}\right)\\ \sin\frac{\theta}{2}\left(\kappa+1-2\cos^2\frac{\theta}{2}\right)\end{Bmatrix}+\frac{K_{II}}{2G}\sqrt{\frac{r}{2\pi}}\begin{Bmatrix}\sin\frac{\theta}{2}\left(\kappa+1+2\cos^2\frac{\theta}{2}\right)\\ \cos\frac{\theta}{2}\left(\kappa-1-2\sin^2\frac{\theta}{2}\right)\end{Bmatrix}+\frac{T}{8G}r\begin{Bmatrix}(\kappa+1)\cos\theta\\ (\kappa-3)\sin\theta\end{Bmatrix} \quad (2)$$

where $G = E/2(1+\nu)$ is the shear modulus, E and ν are the Young's modulus and Poisson's ratio of the material respectively, and $\kappa = (3-\nu)/(1+\nu)$ for plane stress or $\kappa = 3-4\nu$ for strain plain.

WILLIAMS' CRACK TIP STRESS EXPANSION

In the Williams' series expansion, crack tip stress fields [10] are expressed as a function of a number of terms in the series, the series coefficients and a polar coordinate system with its origin at the crack tip:

$$\begin{Bmatrix}\sigma_x\\ \sigma_y\\ \tau_{xy}\end{Bmatrix}=\sum_{n=1}^{\infty}\frac{n}{2}A_{In}r^{\frac{n-2}{2}}\begin{Bmatrix}\left[2+(-1)^n+\frac{n}{2}\right]cos\left(\frac{n}{2}-1\right)\theta-\left(\frac{n}{2}-1\right)cos\left(\frac{n}{2}-3\right)\theta\\ \left[2-(-1)^n-\frac{n}{2}\right]cos\left(\frac{n}{2}-1\right)\theta+\left(\frac{n}{2}-1\right)cos\left(\frac{n}{2}-3\right)\theta\\ -\left[(-1)^n+\frac{n}{2}\right]sin\left(\frac{n}{2}-1\right)\theta+\left(\frac{n}{2}-1\right)sin\left(\frac{n}{2}-3\right)\theta\end{Bmatrix}$$
$$-\sum_{n=1}^{\infty}\frac{n}{2}A_{IIn}r^{\frac{n-2}{2}}\begin{Bmatrix}\left[2-(-1)^n+\frac{n}{2}\right]sin\left(\frac{n}{2}-1\right)\theta-\left(\frac{n}{2}-1\right)sin\left(\frac{n}{2}-3\right)\theta\\ \left[2+(-1)^n-\frac{n}{2}\right]sin\left(\frac{n}{2}-1\right)\theta+\left(\frac{n}{2}-1\right)sin\left(\frac{n}{2}-3\right)\theta\\ -\left[(-1)^n-\frac{n}{2}\right]cos\left(\frac{n}{2}-1\right)\theta-\left(\frac{n}{2}-1\right)cos\left(\frac{n}{2}-3\right)\theta\end{Bmatrix} \tag{3}$$

where $A_{I1} = K_I/\sqrt{2\pi}$, $A_{II1} = -K_{II}/\sqrt{2\pi}$ and $A_{I2} = -T/4$. In addition, crack tip displacement fields [11] are defined as:

$$\begin{Bmatrix}u\\ v\end{Bmatrix}=\sum_{n=1}^{\infty}\frac{r^{n/2}}{2G}a_n\begin{Bmatrix}\left[\kappa+\frac{n}{2}+(-1)^n\right]cos\frac{n\theta}{2}-\frac{n}{2}cos\frac{(n-4)\theta}{2}\\ \left[\kappa-\frac{n}{2}-(-1)^n\right]sin\frac{n\theta}{2}+\frac{n}{2}sin\frac{(n-4)\theta}{2}\end{Bmatrix}+\sum_{n=1}^{\infty}\frac{r^{n/2}}{2G}b_n\begin{Bmatrix}-\left[\kappa+\frac{n}{2}-(-1)^n\right]sin\frac{n\theta}{2}-\frac{n}{2}sin\frac{(n-4)\theta}{2}\\ \left[\kappa-\frac{n}{2}+(-1)^n\right]cos\frac{n\theta}{2}+\frac{n}{2}cos\frac{(n-4)\theta}{2}\end{Bmatrix} \tag{4}$$

where $a_1 = K_I/\sqrt{2\pi}$, $b_1 = -K_{II}/\sqrt{2\pi}$ and $a_2 = T/4$.

CJP MODEL

The CJP model is a novel mathematical model developed by Christopher, James and Patterson [9] based on Muskhelishvili complex potentials [12]. The authors postulated that the plastic enclave which exists around the tip of a fatigue crack and along its flanks will shield the crack from the full influence of the applied elastic stress field and that crack tip shielding includes the effect of crack flank contact forces (so-called crack closure) as well as a compatibility-induced interfacial shear stress at the elastic-plastic boundary. In the original formulation of this model, crack tip fields [9] were characterised as:

$$\sigma_x=-\frac{1}{2}(A+4B+8F)r^{-\frac{1}{2}}cos\frac{\theta}{2}-\frac{1}{2}Br^{-\frac{1}{2}}cos\frac{5\theta}{2}-C-\frac{1}{2}Fr^{-\frac{1}{2}}\left[ln(r)\left(cos\frac{5\theta}{2}+3cos\frac{\theta}{2}\right)+\theta\left(sin\frac{5\theta}{2}+3sin\frac{\theta}{2}\right)\right]$$
$$\sigma_y=\frac{1}{2}(A-4B-8F)r^{-\frac{1}{2}}cos\frac{\theta}{2}+\frac{1}{2}Br^{-\frac{1}{2}}cos\frac{5\theta}{2}+H+\frac{1}{2}Fr^{-\frac{1}{2}}\left[ln(r)\left(cos\frac{5\theta}{2}-5cos\frac{\theta}{2}\right)+\theta\left(sin\frac{5\theta}{2}-5sin\frac{\theta}{2}\right)\right] \tag{5}$$
$$\sigma_{xy}=-\frac{1}{2}r^{-\frac{1}{2}}\left(Asin\frac{\theta}{2}+Bsin\frac{5\theta}{2}\right)-Fr^{-\frac{1}{2}}sin\theta\left[ln(r)cos\frac{3\theta}{2}+\theta sin\frac{3\theta}{2}\right]$$

Five coefficients (A, B, C, F, H) are therefore used to define the stress fields around the crack tip. On the other hand, crack tip displacement fields [9] were characterised according to expression (6). In the mathematical analysis, the

assumption $D+F=0$ must be made in order to give an appropriate asymptotic behaviour of the stress along the crack flank. Therefore, crack tip displacement fields are also defined from the same five coefficients.

$$2G(u+iv)=\kappa\left[-2(B+2F)z^{\frac{1}{2}}+4Fz^{\frac{1}{2}}-2Fz^{\frac{1}{2}}ln(z)-\frac{C-H}{4}z\right]-z\left[-(B+2F)\bar{z}^{-\frac{1}{2}}-F\bar{z}^{-\frac{1}{2}}\overline{ln(z)}-\frac{C-H}{4}\right]$$
$$-\left[A\bar{z}^{\frac{1}{2}}+D\bar{z}^{\frac{1}{2}}\overline{ln(z)}-2D\bar{z}^{\frac{1}{2}}+\frac{C+H}{2}\bar{z}\right] \quad (6)$$

The CJP model provides three stress intensity factors to characterise the stress and displacement fields around the crack tip; an opening mode stress intensity factor K_F, a retardation stress intensity factor K_R, a shear stress intensity factor K_S and also gives the T-stress.

K_F is defined from the applied remote load, traditionally characterized by K_I, but is modified by force components derived from the stresses acting across the elastic-plastic boundary and which therefore influence the driving force for crack growth. Thus, K_F is defined by evaluating the stress component σ_y:

$$K_F=\lim_{r\to 0}\left[\sqrt{2\pi r}\left(\sigma_y+2Fr^{-1/2}\ln r\right)\right]=\sqrt{\frac{\pi}{2}}(A-3B-8F) \quad (7)$$

K_R characterises forces applied in the plane of the crack and which provide a retarding effect on fatigue crack growth. Thus, K_R is evaluated from σ_x:

$$K_R=\lim_{r\to 0}\left[\sqrt{2\pi r}\sigma_x\right]=-(2\pi)^{3/2}F \quad (8)$$

Besides the two previous SIFs, the CJP model proposes that a shear term arises from the requirement of compatibility at the elastic-plastic boundary of the plastically deformed crack wake. Therefore, this shear stress intensity factor (K_S) characterises compatibility-induced shear stress along the plane of the crack at the interface between the plastic enclave and the surrounding elastic field. According to this, K_S is defined from the shear stress component σ_{xy}:

$$K_S=\lim_{r\to 0}\left[\sqrt{2\pi r}\sigma_{xy}\right]=\mp\sqrt{\frac{\pi}{2}}(A+B) \quad (9)$$

The T-stress is defined from its components in the x and y directions: $T_x = -C$; $T_y = -H$.

EXPERIMENTAL WORK

A compact tension (CT) specimen (dimensions shown in Fig. 1a) was manufactured from a 1 mm thick sheet of commercially pure titanium and subjected to constant amplitude fatigue loading at a R ratio of 0.6 (P_{min} = 450 N, P_{max} = 750 N).

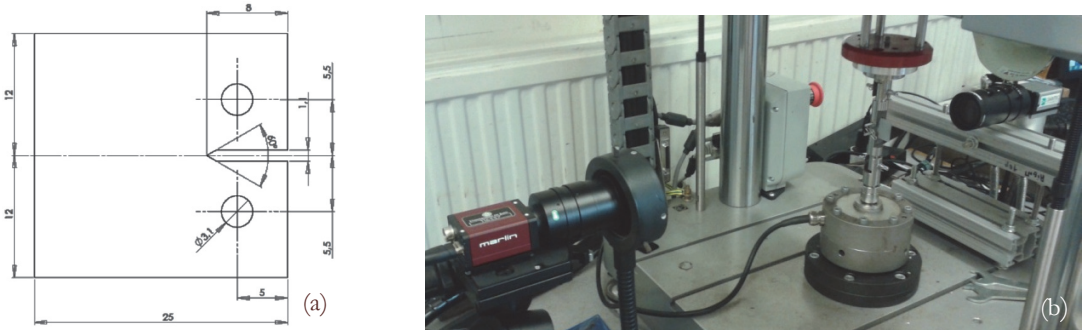

Figure 1: (a) Dimensions (mm) of the CT specimen tested. (b) Experimental set-up used to measure DIC data during fatigue testing.

The two faces of the specimen were prepared for experimental observations in two different ways. The surface to be used for digital image correlation (DIC) was treated by spraying a black speckle with an airbrush over a white background, while the other face was polished to assist in tracking the crack tip with a zoom lens.
Fatigue test was conducted on an ElectroPuls E3000 electric machine (Fig. 1b) at a frequency of 10 Hz. A CCD camera fitted with a macro-zoom lens (MLH-10X EO) to increase the spatial resolution at the region around the crack tip, was placed perpendicular to each face of the specimen. During fatigue testing, the cycling was periodically paused to allow acquisition of a sequence of images at uniform increments through a complete loading and unloading cycle. The CCD camera viewing the speckled face of the specimen was set up so that the field of view was 17.3 x 13 mm (resolution of 13.5 μm/pix) with the crack path located at the centre of the image. Illumination of the surface was provided by a fibre optic ring placed around the zoom lens (shown in Fig. 1b).

EXPERIMENTAL METHODOLOGY

In this section, the two methodologies developed to evaluate the plastic zone size and shape are described. The first methodology is a direct method in which the plastic zone is estimated from the displacement fields determined by experiment, while the second one is an indirect method in which data from experiments is employed in the models to determine the plastic zone size and shape.

Direct method for estimating the plastic zone

This method is based on the application of a yield criterion and consists in identifying the plastic stress field by differentiating the experimentally measured displacement fields. In this work, 2D-DIC has been employed to make experimental displacement measurements. Then, the procedure for implementing this method is described.
The first step in the methodology consists in obtaining the horizontal and vertical displacement fields around the crack tip. In Fig. 2 typical examples of displacement maps are shown for a crack length of 9.40 mm and a load level of 750 N. The developed process will be illustrated using these displacement maps.

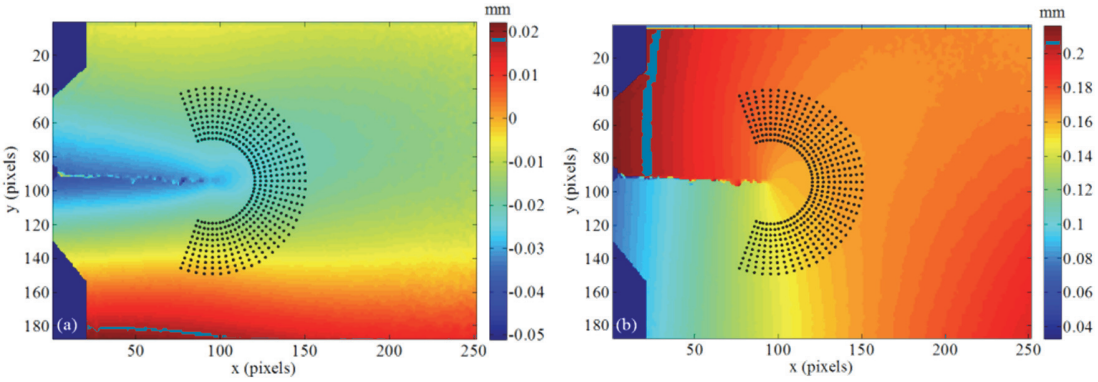

Figure 2: Horizontal (a) and vertical (b) displacement fields measured with DIC for a crack length of 9.40 mm and a load level of 750 N, and data point collection employed for the calculation of stress intensity factors.

The next step in the process involves determining the strain fields at the crack tip by differentiation of the displacement fields. For this purpose, the Green-Lagrange strain tensor [13] is employed because it considers the second order terms and is more accurate than those using only first order terms. Thus, this strain tensor is given by the following expressions:

$$\begin{pmatrix} \varepsilon_{xx} \\ \varepsilon_{yy} \\ \varepsilon_{xy} \end{pmatrix} = \begin{pmatrix} \dfrac{\partial u}{\partial x} \\ \dfrac{\partial v}{\partial y} \\ \dfrac{\partial u}{\partial y} + \dfrac{\partial v}{\partial x} \end{pmatrix} + \frac{1}{2} \begin{pmatrix} \dfrac{\partial u}{\partial x} & 0 & \dfrac{\partial v}{\partial y} & 0 \\ 0 & \dfrac{\partial u}{\partial y} & 0 & \dfrac{\partial v}{\partial y} \\ \dfrac{\partial u}{\partial y} & \dfrac{\partial u}{\partial x} & \dfrac{\partial v}{\partial y} & \dfrac{\partial v}{\partial x} \end{pmatrix} \begin{pmatrix} \dfrac{\partial u}{\partial x} \\ \dfrac{\partial u}{\partial y} \\ \dfrac{\partial v}{\partial x} \\ \dfrac{\partial v}{\partial y} \end{pmatrix} \tag{10}$$

Once the strain fields have been calculated, the next step is to determine the stress fields using Hooke's law. The equivalent stress is calculated from the stress tensor either using the second invariant of the stress deviator (von Mises), or the difference of the maximum and minimum principal stress (Tresca). An estimate of the size and shape of the plastic zone is obtained by connecting all points where the yield criterion is met, i.e., where the equivalent stress is equal to the yield stress. Figs. 3a and 3b show the region of equivalent stress where the value exceeds the yield stress for both the von Mises and Tresca yield criteria. Thus, the plastic zone area can be easily identified from the surrounding elastic field.

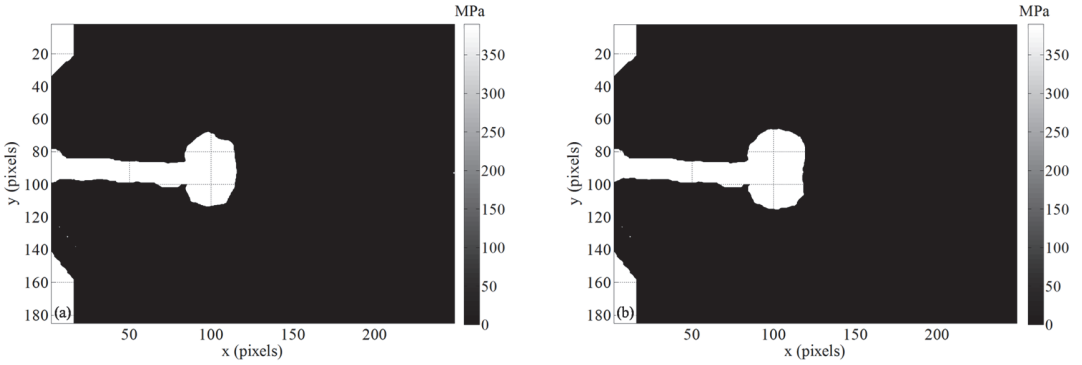

Figure 3: Equivalent stress maps above the yield stress corresponding to von Mises (a) and Tresca (b) criteria for a crack length of 9.40 mm at a load level of 750 N.

In this paper, the area of the plastic zone has been considered as a variable that contains information on both size and shape and which can therefore provide an efficient and powerful technique for making quantitative measurements. Once the plastic zone has been identified, the next step is to characterise its size by quantifying its area at the crack tip. Initially, a set of data points that define the equivalent yield stress contour of the plastic zone must be detected (Fig. 4a). Next, a triangulation function is applied to define the area enclosed by these data points (Fig. 4b). Finally, the plastic zone area can be calculated as the sum of the areas of all the triangles previously defined in the triangulation process.

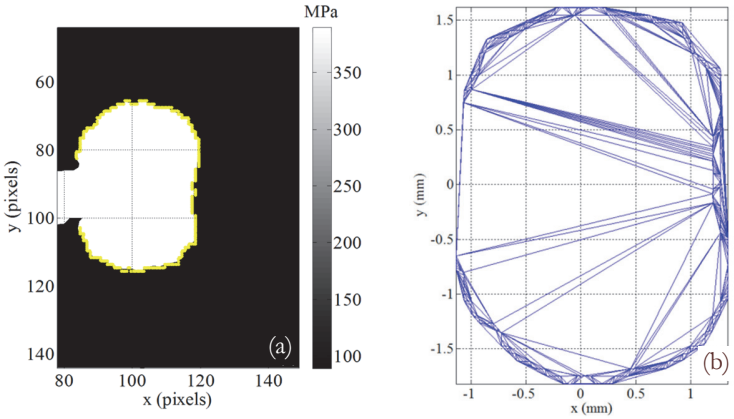

Figure 4: (a) Detection of the data points defining the contour of the plastic zone. (b) Triangulation of the enclosed area for the selected contour.

Indirect method for estimating the plastic zone

The plastic zone estimated from experimental data will be compared with that predicted by the analytical models defining crack tip fields to validate the proposed methodology.

In the literature, the two most popular methods used to estimate the plastic zone size are the Irwin and Dugdale approaches. Both approaches lead to simple estimates for crack tip plastic zone size based on elastic solutions. Therefore, it is more useful to estimate the size and shape of the plastic zone at all angles around the crack tip by applying a yield criterion to an analytical model that describes crack tip stress field. In this work, the three models described in the second will be used to find the plastic zone shape.

The first step in this indirect method consists in determining the stress intensity factors in each crack tip stress model from analysis of the experimental displacement fields. The multi-point over-deterministic method developed by Sanford

and Dally [14] forms the basis for this process. The models are valid only for the elastic field near the crack tip singularity and hence it was necessary to identify the near-tip zone where valid experimental data could be obtained. An annular mesh (Fig. 2) was defined to establish the region from which determining the SIFs. Two parameters are fundamentals for defining the annular mesh: inner and outer radii. The inner radius was defined with sufficient extent to avoid including plastic deformation at the crack tip, while the outer radius was defined to be within the singularity dominated zone.
From the calculation of the stress intensity factors, the coefficients defining the crack tip fields in the analytical models can be extracted to found the plastic zone contour. Crack tip stress fields in the analytical models depend on a set of coefficients and the coordinates of the analysed data points. Therefore, an expression as a function of the above parameters for the equivalent stress according to a yield criterion can be obtained. From this expression, an error function is defined as the difference between the equivalent stress and the yield stress of the material. Thus, plastic zone contour is found from the evaluation of the error function by analysing angle values between 0º and 360º to estimate the radius of the plastic zone. Hence the size and shape of the experimentally determined plastic zone can be compared with that found using the three different theoretical models that describe the crack tip stress and displacement fields.

RESULTS AND DISCUSSION

Fig. 5 shows size and shape data obtained for the plastic zone at maximum load using the von Mises yield criterion for two different crack lengths (6.42 and 9.20 mm). The white area represents the experimental plastic zone estimated from the direct method, while the dotted contours correspond to the plastic zone found for the three models by implementing the indirect method using the model coefficients. It is clear that the plastic zone size and shape predicted by the CJP model is an excellent fit to the experimental data, while the Westergaard and Williams models predict somewhat larger dimensions. Therefore, from a qualitative point of view, the CJP model seems that shows a great potential to predict the plastic zone at the crack tip.

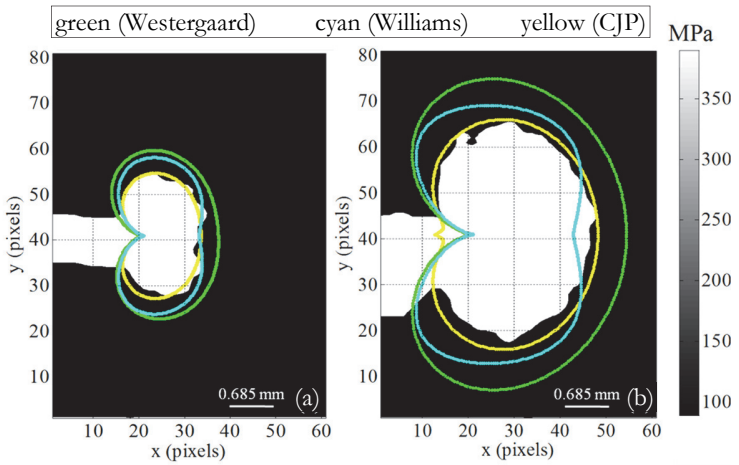

Figure 5: Comparison between the experimental plastic zone shape and that predicted by the models using the von Mises criterion for two crack lengths, (a) 6.42 and (b) 9.20 mm at maximum load.

Moreover, as indicated above the plastic zone area is evaluated for its quantification. Fig. 7 shows the evolution of both experimental and predicted plastic zone area with the crack length using the von Mises yield criterion. Again, the experimental data is in close agreement with the plastic zone area calculated from the CJP model at all crack lengths, while the predicted area using the Westergaard and Williams models is higher than the experimental results. The Westergaard model shows a progressively larger error as the crack length increases while the error in the Williams solution remains fairly constant. It can be concluded that the CJP model provides an improved prediction of the crack tip plastic zone area and shape compared with either the Westergaard or Williams models.
Fig. 6 illustrates the difference that choice of yield criterion (von Mises or Tresca) would make to the experimental and CJP predictions of plastic zone area. As expected, sizes predicted using the Tresca criterion are higher, but close agreement is still observed between the experimental predictions and those provided by the CJP model.

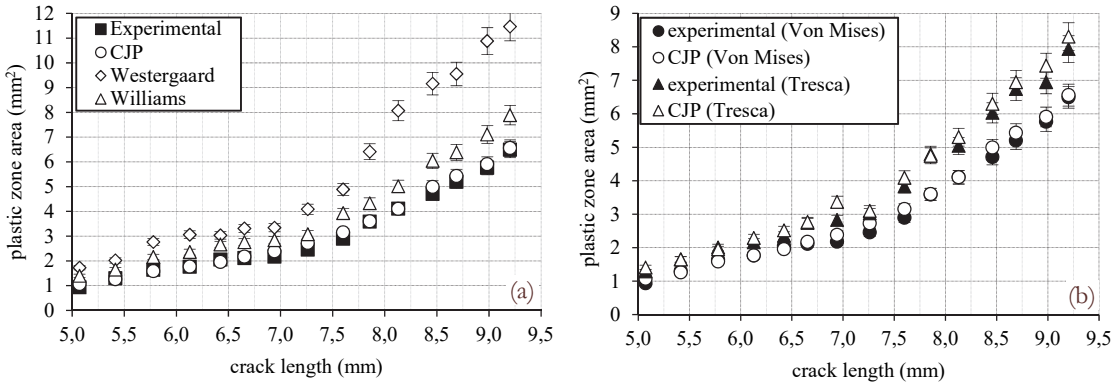

Figure 6: (a) Comparison between the experimental and model predictions of plastic zone area at maximum applied load as a function of the crack length using the von Mises criterion. (b) Comparison between the experimental and CJP model predictions of plastic zone size at maximum load using both the von Mises and Tresca yield criteria.

CONCLUSIONS

In the present paper a novel experimental methodology for the quantitative evaluation of the crack tip plastic zone size during fatigue crack growth has been presented. This methodology uses differentiation of the measured displacement fields to obtain strain maps that can be combined with a yield criterion to estimate the shape and size of the crack tip plastic zone. These predictions can be compared with estimates of the plastic zone size obtained from analytical models that describe crack tip displacement fields. This work indicates that the CJP model provides the best prediction of the crack tip plastic zone shape and size. It is proposed that this agreement supports the fact that the CJP model, through its basic assumptions regarding the influences of plasticity on the elastic stress fields ahead of the crack tip, is better at defining the real size of the plastic zone.

ACKNOWLEDGEMENTS

The current work has been conducted with the financial support from Gobierno de España through the project 'Proyecto de Investigación de Excelencia del Ministerio de Economía y Competitividad MAT2016-76951-C2-1-P'.

REFERENCES

[1] Uguz, A., Martin, J.W., Plastic zone size measurement techniques for metallic materials, Materials Characterization, 37 (1996) 105–118.

[2] Steuwer, A., Edwards, L., Pratihar, S., Ganguly, S., Peel, M., Fitzpatrick, E.M., Marrow, T.J., Withers, P.J., Sinclair, I., Singh, K.D., Gao, N., Buslaps, T., Buffière, J.Y., In situ analysis of cracks in structural materials using synchrotron X-ray tomography and diffraction, Nuclear Instruments and Methods, in Physics Research Section B: Beam Interactions with Materials and Atoms, 246 (2006) 217–225.

[3] Nowell, D., Kartal, M.E., de Matos, P.F.P., Digital image correlation measurement of near-tip fatigue crack displacement fields: constant amplitude loading and load history effects, Fatigue and Fracture of Engineering Materials and Structures, 36(1) (2013) 3–13.

[4] Díaz, F.A., Patterson, E.A., Yates, J.R., Assessment of effective stress intensity factors using thermoelastic stress analysis, The Journal of Strain Analysis for Engineering Design, 44 (2009) 621–631.

[5] Wright, S.I., Nowell, M.M., Field, D.P., A review of strain analysis using electron backscatter diffraction, Microscopy and Microanalysis, 17 (2011) 316–329.

[6] Irwin, G.R., Analysis of stresses and strains near the end of a crack traversing a plate, Journal of Applied Mechanics, 24 (1957) 361–364.

[7] Dugdale, D.S., Yielding in steel sheets containing slits, Journal of the Mechanics and Physics of Solids, 8 (1960) 100–104.
[8] Janssen, M., Zuidema, J., Wanhill, R.J.H., Fracture Mechanics, Spon Press, (2006).
[9] James, M.N., Christopher, C.J., Lu, Y., Patterson, E.A., Local crack plasticity and its influence on the global elastic field, International Journal of Fatigue, 46 (2013) 4–15.
[10] Ramesh, K., Gupta, S., Kelkar, A.A., Evaluation of stress field parameters in fracture mechanics by photoelasticity–Revisited, Engineering Fracture Mechanics, 56 (1997) 25–45.
[11] Yates, J.R., Zanganeh, M., Tai, Y.H., Quantifying crack tip displacement fields with DIC, Engineering Fracture Mechanics, 77 (2010) 2063–2076.
[12] Muskhelishvili, N.I., Some Basic Problems of the Mathematical Theory of Elasticity, Nordhoff International Publishing, (1977).
[13] Singh, A.K., Mechanics of Solids, Prentice-Hall of India Private Limited, (2010).
[14] R.J. Sanford, J.W. Dally, A general method for determining mixed-mode stress intensity factors from isochromatic fringe patterns, Engineering Fracture Mechanics, 11 (1979) 621–633.